S=1 axial next-nearest neighbour Ising (ANNNI) model with higher order spin interaction

1993 J. Phys. A: Math. Gen. 26 1811

(http://iopscience.iop.org/0305-4470/26/8/010)

J. Phys. A: Math. Gen. 26 (1993) 1811-1821. Printed in the UK

$S = 1$ axial next-nearest neighbour Ising (ANNNI) model with higher order spin interaction

Y Muraoka†, M Ochiai‡, T Idogaki‡ and N Uryû§

† Department of General Education, Ariake National College of Technology, Omuta, Fukuoka 386, Japan

‡ Department of Applied Science, Faculty of Engineering 36, Kyusyu University, Fukuoka 812, Japan

§ Laboratory of Applied Physics, Faculty of Engineering, Nagasaki University, Nagasaki 852, Japan

Received 22 October 1992

Abstract. The three-dimensional $S = 1$ axial next-nearest neighbour Ising (ANNNI) model is discussed. In addition to the ferromagnetic intra- and inter-layer interactions J_0 and J_1, two types of competing antiferromagnetic interactions are considered between next-nearest layers, i.e. ordinary two-site two-spin interaction, $J_2 S_i S_{i+2}$, ([2-2] model) or three-site four-spin interaction, $J_3 S_i S_{i+1}^2 S_{i+2}$, ([3-4] model). For both models, the ground state is rigorously obtained by means of the transfer matrix method, and proved to change from ferromagnetic to antiphase spin structure at J_2(or J_3)$/J_1 = -\frac{1}{2}$ with the increase of competition. From magnetization, internal energy, specific heat and 'absolute magnetization' calculated by the Monte Carlo simulation with Fourier transformation, phase boundaries among paramagnetic, ferromagnetic and modulated phases are determined with location of the Lifshitz point. It is confirmed that for the [3-4] model the selfspin correlation, S_{i+1}^2, included in three-site four-spin interaction weakens the frustration between J_1 and J_3 at high temperatures. In the vicinity of the paramagnetic phase transition, the correlation along the z-direction becomes considerably weaker than the correlation in xy-plane owing to the frustration along the z-direction. Consequently, for both [2-2] and [3-4] model there exists the temperature region in which the system behaves as quasi two-dimensional system.

1. Introduction

The axial next-nearest neighbour Ising (ANNNI) model [1, 2] is a particularly simple model exhibiting spatially modulated phases which can be either commensurate or incommensurate with the underlying lattice. Originally, the ANNNI model was introduced by Elliot [1] and, Bak and von Boehm [2] to describe the sinusoidally modulated phases of the rare-earth metals or rare-earth intermetallic compounds such as Er [3] and CeSb [4]. Due to a large axial anisotropy of rare-earth elements, these spins behave as Ising spin of spin value S ($S \geq \frac{1}{2}$). The molecular-field calculation [2, 5], the Monte Carlo simulation [6], the high temperature series expansion [7, 8] performed mainly for $S = \frac{1}{2}$ system have revealed the interesting properties such as the 'devil's staircase' and partially disordered phase.

In the case of $S \geq 1$, it is known that not only the ordinary bilinear exchange interaction, $S_i S_j$, but also the higher order spin interactions, $S_i^2 S_j^2$, $S_i S_j^2 S_k$ and so on, become important. These higher order spin interactions originate from the magnetostriction or can be derived from the higher order perturbation procedure. The role and the importance of those interactions have been discussed extensively by many investigators

0305-4470/93/081811+11$07.50

[9]. Particularly, in the previous work for the magnetically dilute Ising system [10], the characteristic difference between the three-site-type interaction, $S_iS_j^2S_k$, and the two-site-type interaction, S_iS_j, has been emphasized in the concentration dependence of the Curie temperature. Recently, the ANNNI model with higher order spin interactions has been studied by Nakanishi [11], replacing the four-spin correlation function by the product of the thermal average of each spin and calculating the entropy based on the two level model. The higher order spin interaction in their work corresponds to the four-site-type interaction, $S_iS_jS_kS_l$, for $S=\frac{1}{2}$ and the three-site-type interaction, which is peculiar to $S \geqslant 1$, is not considered.

In this paper, based on the transfer matrix method and the Monte Carlo simulation, we discuss the ground state and the order-disorder transition for two types of the three-dimensional $S=1$ ANNNI model. The first one is the ordinary model described by the following Hamiltonian:

$$H = -J_0 \sum_{\langle i,j \rangle}^{nn} S_iS_j - J_1 \sum_{\langle i,j \rangle}^{nn} S_iS_j - J_2 \sum_{\langle i,j \rangle}^{nnn} S_iS_j \tag{1}$$

where $S_i = \pm 1$ or 0, $J_0 > 0$ is a ferromagnetic nearest-neighbour interaction within the xy-plane, and $J_1 > 0$ and $J_2 < 0$ are competing interactions between nearest- and next-nearest layers perpendicular to the z-direction, respectively (figure 1). The second one is the model, in which the two-site two-spin interaction, $J_2S_iS_j$, is replaced by three-site four-spin interaction, $J_3S_iS_j^2S_k$, among three adjacent layers, i.e.

$$H = -J_0 \sum_{\langle i,j \rangle}^{nn} S_iS_j - J_1 \sum_{\langle i,j \rangle}^{nn} S_iS_j - J_3 \sum_{\langle i,j,k \rangle}^{nnn} S_iS_j^2S_k. \tag{2}$$

In the following, these two models are termed [2-2] model and [3-4] model, respectively, and discussed comparatively.

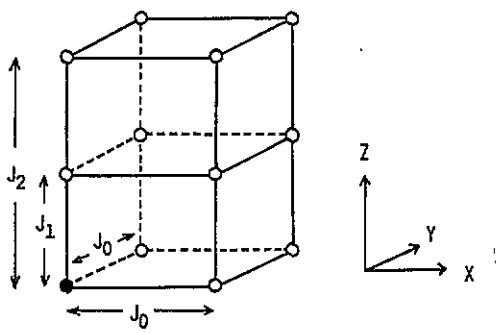

Figure 1. The three-dimensional ANNNI model.

The arrangement of the paper is as follows. In section 2, the ground state and the ground state energy for [2-2] and [3-4] models are rigorously calculated using the transfer matrix method. In section 3, the phase transitions at finite temperature are discussed for both models by the Monte Carlo simulations with Fourier transformation. Finally, in section 4 the results are summarized and the concluding remarks are given.

2. The spin structures of the ground state of the three-dimensional ANNNI model

The ground state of the three-dimensional ANNNI model can be understood by studying the spin configurations of the one-dimensional Ising system along the z-direction

(competing direction) described by the Hamiltonian

$$H_{1d} = -\sum_i (J_1 S_i S_{i+1} + J_2 S_i S_{i+2} + J_3 S_i S_{i+1}^2 S_{i+2}) \tag{3}$$

where $S_i = \pm 1$ or 0. We have investigated the spin configurations by the transfer matrix method [12]. In the case of N spin system with the periodic boundary condition, $S_{N+i} = S_i$, the partition function is given by

$$Z_N = \sum_{\{S\}} \prod_{i=1}^{N} L(S_i, S_{i+1}, S_{i+2}) \tag{4}$$

where

$$L(S_i, S_{i+1}, S_{i+2}) = e^{K_1 S_i S_{i+1} + K_2 S_i S_{i+2} + K_3 S_i S_{i+1}^2 S_{i+2}} \tag{5}$$

Σ means the trace for each spin, and $K_i = J_i / T (i = 1 \sim 3)$. We introduce the variables, $\tau_i = (S_i, S_{i+1})$, as the bases of the direct product space for two neighbouring spins, where τ_i has nine sets, (1, 1), (1, 0), (1, −1), (0, 1), (0, 0), (0, −1), (−1, 1), (−1, 0) and (−1, −1). Using these bases, equation (4) is represented in the following

$$Z_N = \sum_{\{\tau\}} \prod_{i=1}^{N} L(\tau_i, \tau_{i+1}) = \mathrm{Tr}\, \boldsymbol{L}^N \tag{6}$$

where $\boldsymbol{L}$ is the 9×9 transfer matrix describing $L(\tau_i, \tau_{i+1}) = L(S_i, S_{i+1}, S_{i+2})$ with bases τ. With the maximum eigenvalue λ_1 of nine eigenvalues, λ_i $(i = 1 \sim 9)$, of the transfer matrix $\boldsymbol{L}$, one can express the free energy as

$$F = -T \ln \left\{ \lambda_1^N \left[1 + \sum_{i=2}^{9} \left(\frac{\lambda_i}{\lambda_1} \right)^N \right] \right\}. \tag{7}$$

In the limit $N \to \infty$, the ground state energy per spin is given by the following equation:

$$E = -T \ln \lambda_1. \tag{8}$$

From equation (5), $\boldsymbol{L}$ is written as

$$\boldsymbol{L} = \begin{pmatrix} \boldsymbol{L}_{11} & \boldsymbol{L}_{12} & \boldsymbol{L}_{13} \\ \boldsymbol{L}_{21} & \boldsymbol{L}_{22} & \boldsymbol{L}_{23} \\ \boldsymbol{L}_{31} & \boldsymbol{L}_{32} & \boldsymbol{L}_{33} \end{pmatrix} \tag{9}$$

where the 3×3 matrices $\boldsymbol{L}_{ij}$ $(i, j = 1 \sim 3)$ are given by

$$\boldsymbol{L}_{11} = \begin{pmatrix} e^{K_1 + K_2 + K_3} & e^{K_1} & e^{K_1 - K_2 - K_3} \\ 0 & 0 & 0 \\ 0 & 0 & 0 \end{pmatrix} \tag{10}$$

$$\boldsymbol{L}_{12} = \begin{pmatrix} 0 & 0 & 0 \\ e^{K_2} & 1 & e^{-K_2} \\ 0 & 0 & 0 \end{pmatrix} \tag{11}$$

$$\boldsymbol{L}_{13} = \begin{pmatrix} 0 & 0 & 0 \\ 0 & 0 & 0 \\ e^{-K_1 + K_2 + K_3} & e^{-K_1} & e^{-K_1 - K_2 - K_3} \end{pmatrix} \tag{12}$$

and the other ones L_{21}, L_{22} and L_{23} are obtained by putting $K_i = 0$, and L_{31}, L_{32} and L_{33} are obtained by putting $K_i \to -K_i$ in equations (10), (11) and (12), respectively.

We write down the eigenequation from equation (9),

$$\mathrm{Det}|L - \lambda E| = \sum_{n=0}^{9} C_n \lambda^n = 0 \tag{13}$$

where C_n are analytically obtained as the function of K_i. At zero temperature K_i are infinite. Therefore, in order to determine the maximum eigenvalue λ_1, one can neglect all terms except λ^9 and the maximum term in the remaining part of equation (13). For arbitrary κ_2 (or κ_3), where $\kappa_2 = J_2/J_1$, $\kappa_3 = J_3/J_1$ and $J_1 > 0$, the maximum eigenvalue λ_1 has been obtained;

- [2-2] model: $J_3 = 0$
  For $\kappa_2 \geqslant -\frac{1}{2}$, $\lambda_1 = \exp(K_1 + K_2)$ and for $\kappa_2 \leqslant -\frac{1}{2}$, $\lambda_1 = \exp(-K_2)$. From equation (8), the ground state energy is
  $$E = \begin{cases} -J_1 - J_2 & (\kappa_2 \geqslant -\frac{1}{2}) \\ J_2 & (\kappa_2 \leqslant -\frac{1}{2}) \end{cases}$$
  corresponding to the ferromagnetic phase ($\uparrow\uparrow\uparrow\uparrow$) and antiphase ($\uparrow\uparrow\downarrow\downarrow$), respectively.
- [3-4] model: $J_2 = 0$
  $$E = \begin{cases} -J_1 - J_3 & (\kappa_3 \geqslant -\frac{1}{2}) \\ J_3 & (\kappa_3 \leqslant -\frac{1}{2}). \end{cases}$$

Consequently, in both models as competition increases between nearest and next-nearest neighbour interaction, the ferromagnetic phase changes into the antiphase at $\kappa_2^c = \kappa_3^c = -\frac{1}{2}$. This result is in agreement with that of the three-dimensional $S = \frac{1}{2}$ ANNNI model [6].

3. The Monte Carlo simulation

For $J_0 = J_1 > 0$, $J_2, J_3 < 0$, the Monte Carlo simulation [13, 14] is performed for the $L \times L \times L_z$, $(L, L_z) = (6, 40)$, simple cubic lattice with periodic boundary condition in three directions [6]. The magnetization per spin;

$$M = \frac{1}{N} \sum_i^z \sum_i^{xy} S_i \tag{14}$$

internal energy E, specific heat C and 'absolute magnetization' defined by

$$M_a = \frac{1}{N} \sum_i^z \left| \sum_i^{xy} S_i \right| \tag{15}$$

are calculated. In the above, N is the number of spins, and the first and second summations denote the sum along the z-direction and in the xy-plane, respectively. In antiphase and modulated phase, M is expected to be zero but M_a is not the case owing to the ferromagnetic order in xy-plane, and in the paramagnetic phase both M and M_a should be zero. Therefore, M_a may be regarded as the order parameter of ferromagnetic ordering in the xy-plane. The specific heat is calculated using the fluctuation-dissipation relation as

$$C = \frac{\langle H^2 \rangle - \langle H \rangle^2}{T^2}. \tag{16}$$

The spin structures in the z-direction are analysed by checking the Fourier transformation coefficients

$$a_{q_z} = \frac{2}{L_z} \sum_{z=1}^{L_z} M(z) \cos(q_z \cdot z) \tag{17}$$

$$b_{q_z} = \frac{2}{L_z} \sum_{z=1}^{L_z} M(z) \sin(q_z \cdot z) \tag{18}$$

where $M(z)$ denotes the layer magnetization per spin:

$$M(z) = \frac{1}{L^2} \sum_{i}^{xy} S_i. \tag{19}$$

The calculations are mainly carried out for heating process. To establish an equilibrium the first 1500–12 000 MCS (Monte Carlo Steps per spin) are discarded and the same order of MCS are used to calculate the thermal averages. The initial states used are ferromagnetic state for κ_2(or κ_3) $> -\frac{1}{2}$ and antiphase state for κ_2(or κ_3) $< -\frac{1}{2}$.

The dependence of the wavevector q_z on temperature for κ_2(or κ_3) $= -0.52$, -0.8 is shown in figure 2. In both models, the wavevector behaves like the 'devil's staircase'. The temperatures, T_{FU} and T_{FL}, are determined from the dependence of the wavevector on temperature. The upper temperature, T_{FU}, is the temperature at which all Fourier coefficients almost vanish within the numerical precision. Namely, the long range correlation along the z-direction is strongly suppressed in $T > T_{FU}$. The lower temperature, T_{FL}, is the temperature at which the wavevector with maximum Fourier coefficient jumps from the ground state wavevector to another wavevector. Namely, T_{FL} corresponds to the transition temperature from the ground state to a modulated phase. The obtained critical wavevectors at $T = T_{FU}$ for some κ_2(or κ_3) are shown in figure 3.

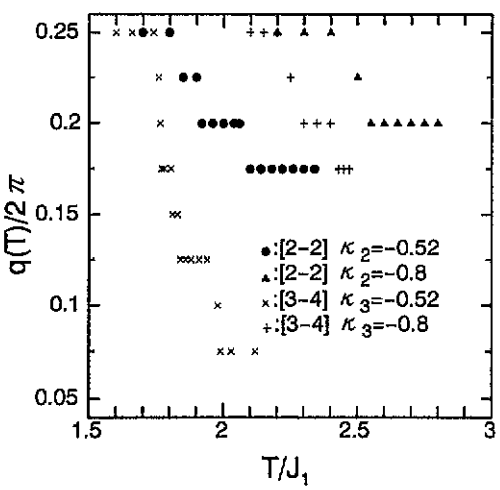

Figure 2. The dependence of the wavevector q_z on temperature. ● and ▲ denote the case of $\kappa_2 = -0.52$ and -0.8 for [2-2] model, and × and + denote the case of $\kappa_3 = -0.52$ and -0.8 for [3-4] model.

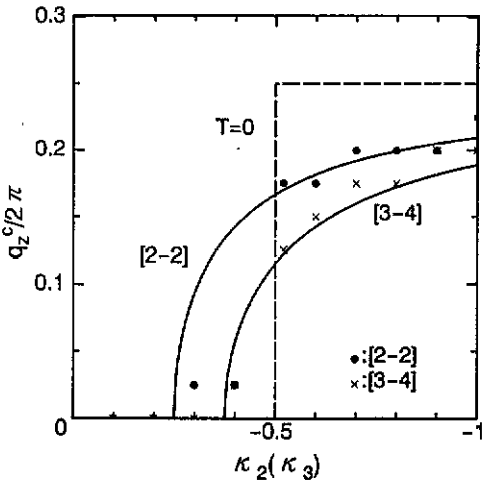

Figure 3. The dependence of the critical wavevector q_z^c on κ_2 (or κ_3) for [2-2] and [3-4] model. ● and × denote the results by means of the Monte Carlo simulation for [2-2] and [3-4] model, respectively. Solid lines denote the results by means of the molecular-field approximation in the appendix. Ground state is shown by dashed line.

The specific heat and the internal energy of the [3-4] model for $\kappa_3 = -0.6$ and -0.2 are shown in figure 4. There exist two peaks in the plot of specific heat for $\kappa_3 = -0.6$ (figure 4(a)). Let us define the lower and the upper temperature corresponding to these two peaks as T_L and T_U, respectively. As κ_3 approaches to -1.0, the interval between T_L and T_U becomes narrow. For $-0.3 \leq \kappa_3$ two peaks collapse into a single peak, i.e. $T_L = T_U$ (figure 4(b)). The [2-2] model shows similar behaviours of specific heat and internal energy as the [3-4] model.

The magnetization (M) and the 'absolute magnetization' (M_a) of the [3-4] model for $\kappa_3 = -0.6$ and -0.2 are shown in figure 5. For $\kappa_3 = -0.6$, M is almost zero in the whole range of temperature and M_a shows a drastic change suggesting the first order transition (figure 5(a)). On the other hand, for $\kappa_3 = -0.2$, both M and M_a show the

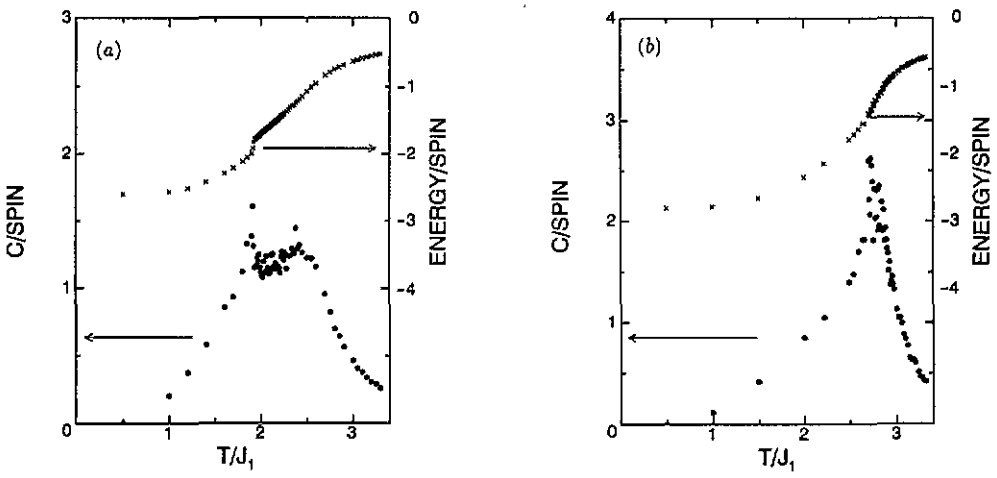

Figure 4. Specific heat (●) and internal energy (×) per spin for [3-4] model. (a): $\kappa_3 = -0.6$ and (b): $\kappa_3 = -0.2$, respectively.

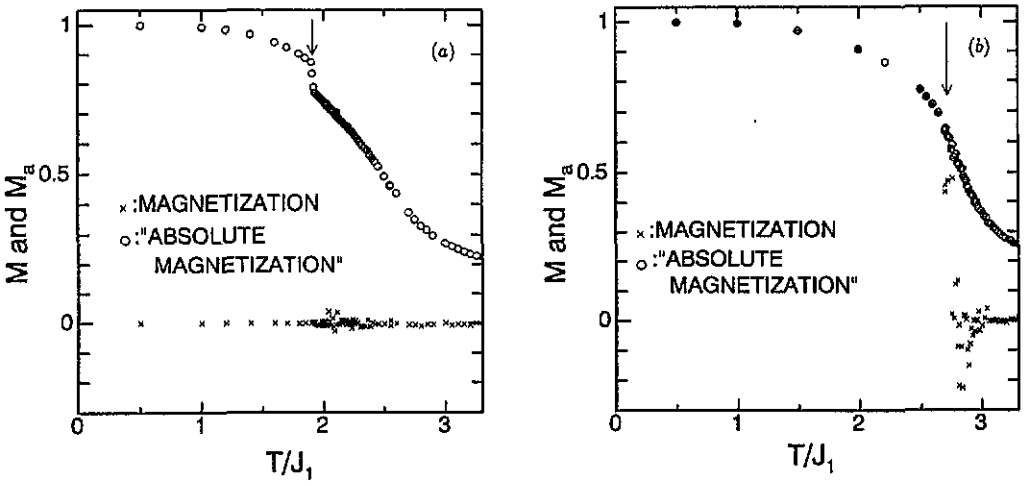

Figure 5. Magnetization (×) and 'absolute magnetization' (○) per spin for [3-4] model. (a): $\kappa_3 = -0.6$ and (b): $\kappa_3 = -0.2$, respectively.

drastic change at the same temperature (figure 5(*b*)). In both cases, the position of the drastic change is in agreement with the above defined T_L. At T_U, both M and M_a do not show any remarkable behaviour, while the position of inflection point in M_a versus T/J_1 may correspond to T_U. The [2-2] model shows similar behaviours of M and M_a as the [3-4] model.

From the above results, the $T-\kappa_2$ (or κ_3) magnetic phase diagrams for [2-2] and [3-4] model have been obtained and are shown in figures 6 and 7, respectively. T_{FU} and T_{FL} are determined by the dependence of the wavevector on temperature, and T_U and T_L are determined by specific heat C and magnetization M and M_a. In the calculation, T_L is in agreement with T_{FL} within a limit of the error, and this $T_L(=T_{FL})$ may correspond to the transition temperature from the ground state to a modulated phase. On the other hand, T_{FU} is different from T_U. Figure 6 and figure 7 suggest an inequality, $T_{FU} \leqslant T_U$. In the vicinity of T_{FU}, the correlation along the z-direction becomes considerably weaker than the correlation in the xy-plane owing to the frustration along the z-direction, and until T_U is approached no apparent anomaly is found in the specific heat C, magnetization M and M_a. This suggests that in $T_{FU} < T < T_U$ the present system behaves like a quasi two-dimensional ferromagnetic one and that T_U corresponds to the transition to the paramagnetic phase. Figure 8 shows the 'absolute magnetization' versus T/T_{FU} for $\kappa_3 = -0.52$, -0.8 and -1.0. Near $T \sim T_{FU}$, M_a is finite and as κ_3 approaches -0.5, M_a becomes larger. Namely, near $T \sim T_{FU}$ as the competition along the z-direction becomes stronger, the correlation in the xy-plane remains stronger than the correlation along the z-direction. This result supports the above mentioned quasi two-dimensional behaviour. This quasi two-dimensional behaviour may be related to a smooth crossover in the effective susceptibility index [15].

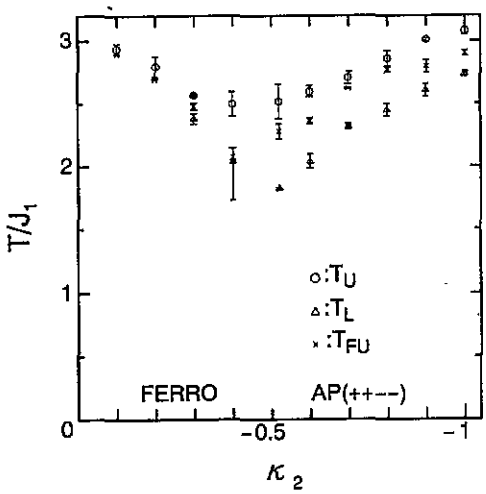

Figure 6. The magnetic phase diagram for [2-2] model. ○, △ and × denote T_U, $T_L(=T_{FL})$ and T_{FU}, respectively.

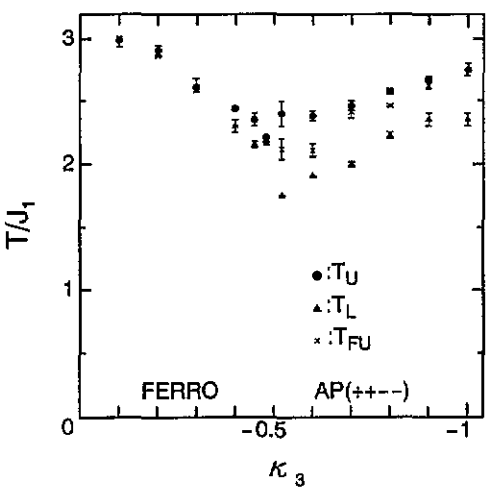

Figure 7. The magnetic phase diagram for [3-4] model. ●, ▲ and × denote T_U, $T_L(=T_{FL})$ and T_{FU}, respectively.

Letting all interactions along the z-direction be zero, both [2-2] and [3-4] models result in $S=1$ Ising model on a square lattice. From the Monte Carlo simulation on three lattices (6×6, 15×15 and 20×20), we obtained $T_c/J_0 \sim 1.8$ as the transition temperature of this model. As κ_2 (or κ_3) approaches -0.5, the frustration along the

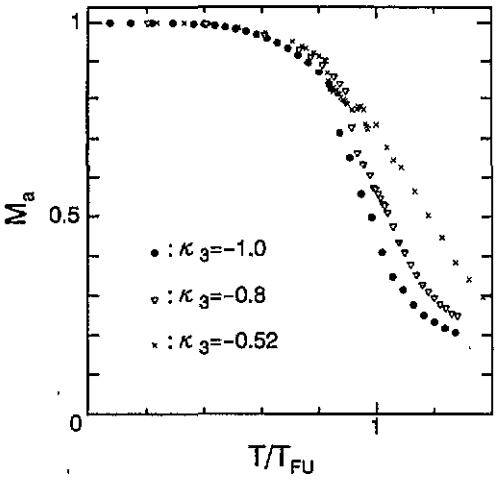

Figure 8. 'Absolute magnetization' per spin versus T/T_{FU} for [3-4] model. ●, ▽ and × denote the case of $\kappa_3 = -1.0$, -0.8 and -0.52.

z-direction becomes strong, the transition temperature T_U/J_1 lowers to 2.3. This lowering of the transition temperature may be attributed to the quasi two-dimensional behaviour due to the frustration along the z-direction.

For both models, consequently, there exists the single transition of F→P for κ_2 (or κ_3) $> \kappa_2^*$ (or κ_3^*), and successive transition of F→M→P or A→M→P for κ_2 (or κ_3) $\leqslant \kappa_2^*$ (or κ_3^*), where F, A, M and P denote the ferromagnetic phase, the antiphase, the modulated phase and the paramagnetic phase, respectively. The Lifshitz point LP: (κ_2^* (or κ_3^*), T^*) at which these three phases of F, M and P coexist is estimated as follows

$$-0.3 \leqslant \kappa_2^* \leqslant -0.2 \qquad 2.57 \leqslant T^*/J_1 \leqslant 2.8 \qquad \text{for [2-2] model}$$

$$-0.45 \leqslant \kappa_3^* \leqslant -0.3 \qquad 2.35 \leqslant T^*/J_1 \leqslant 2.61 \qquad \text{for [3-4] model.}$$

For comparison, the estimates of LP by simple molecular field calculation is given in table 1.

Phase diagrams for the [3-4] model are compared with that of the [2-2] model in figure 9. Order-disorder line (T_U-line) of the two models crosses near κ_2 (or κ_3) $= -0.3$. This crossing is explained by a selfspin correlation S_j^2 included in three-site four-spin interaction, $J_3 S_i S_j^2 S_k$. For κ_2 (or κ_3) $\geqslant -0.5$, the ground ferromagnetic state is stabilized by ferromagnetic nearest-neighbour interaction, J_1, and disturbed by antiferromagnetic

Table 1. T_c, T_m and Lifshitz point for $S = 1$ ANNNI model by means of the molecular-field approximation in the appendix, where $\kappa_0 = J_0/J_1$ and $a = S(S+1)/3 = \frac{2}{3}$. The transition temperature T_U defined in section 3 corresponds to T_c or T_m in this table.

	T_c/aJ_1	T_m/aJ_1	Lifshitz point
[2-2] model	$4\kappa + 2 + 2\kappa_2$	$4\kappa_0 - 2\kappa_2 - \dfrac{1}{4\kappa_2}$	$\kappa_2^* = -\frac{1}{4}$
[3-4] model	$4\kappa_0 + 2 + \dfrac{4\kappa_3}{3}$	$4\kappa_0 - \dfrac{4\kappa_3}{3} - \dfrac{3}{8\kappa_3}$	$\kappa_3^* = -\frac{3}{8}$

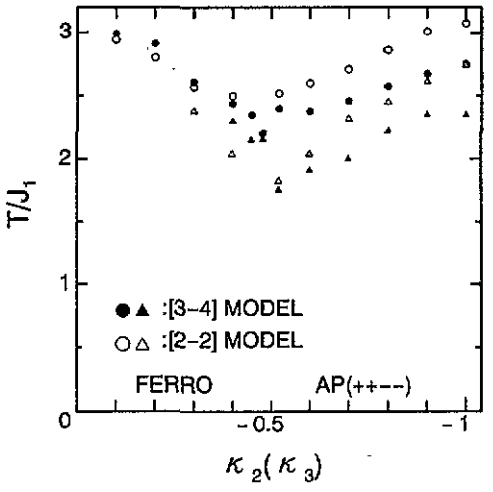

Figure 9. The magnetic phase diagram for [2-2] (○, △) and [3-4] (●, ▲) model without error bar.

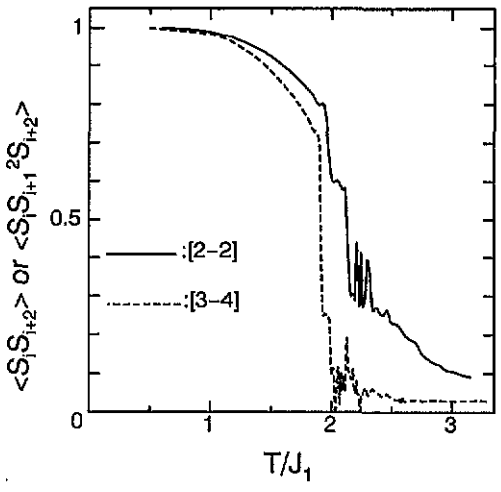

Figure 10. The temperature dependence of the spin correlation for κ_2 (or κ_3) = −0.6. Solid and dashed lines denote $\langle S_iS_{i+2}\rangle$ for [2-2] model and $\langle S_iS_{i+1}^2S_{i+2}\rangle$ for [3-4] model, respectively.

next-nearest-neighbour interaction, J_2 or J_3. As the temperature is raised, the three-site four-spin interaction, $J_3S_iS_j^2S_k$, is expected to be diminished by the factor S_j^2 compared with bilinear interaction, $J_2S_iS_j$. This means that the frustration effect for the [3-4] model is weaker at high temperatures and T_U becomes higher than the [2-2] model. On the other hand, for κ_2 (or κ_3) < -0.5, the ground antiphase state and the modulated phase are stabilized by antiferromagnetic next-nearest-neighbour interaction, J_2 or J_3, and disturbed by ferromagnetic nearest-neighbour interaction, J_1. Therefore, for the same reason as the above case, both T_U and T_L for the [2-2] model are higher than those for the [3-4] model. Figure 10 shows the dependence of $\langle S_iS_{i+2}\rangle$ and $\langle S_iS_{i+1}^2S_{i+2}\rangle$ on temperature for κ_2 (or κ_3) = −0.6 by means of the Monte Carlo simulation. Figure 10 supports the above discussion.

4. Conclusions

We have presented the results of a study of both [2-2] and [3-4] models in three-dimensions, based on the transfer matrix method and the Monte Carlo simulation.

By the transfer matrix method, the ground states of two models have been rigorously determined. Both models have common ground states for arbitrary κ_2 (or κ_3). For κ_2 (or κ_3) > -0.5, the ground state is ferromagnetic state, and for κ_2 (or κ_3) < -0.5, the ground state is aintiphase of $q_z/2\pi = \frac{1}{4}$.

By means of the Monte Carlo simulation, some physical quantities and the Fourier coefficients of magnetization have been calculated. From the dependence of these quantities on temperature, T_U, T_{FU}, T_{FL} and the Lifshitz point have been estimated, and the phase diagrams for both models have been obtained. Comparing [2-2] and [3-4] models, it is confirmed that for the [3-4] model the selfspin correlation S_j^2 included in three-site four-spin interaction, weakens the frustration between J_1 and J_3 at high temperatures. In the vicinity of T_{FU} the correlation along the z-direction becomes

considerably weaker than the correlation in the xy-plane owing to the frustration along the z-direction. Consequently, it is confirmed that for both [2-2] and [3-4] models there exists a temperature region in which the system behaves as quasi two-dimensional.

In the Monte Carlo simulation, the $6\times6\times40$ system has been treated. The dependence of the phase boundaries and detailed structure in modulated phase, etc., on the system size are interesting problems to be investigated. It is difficult to use Monte Carlo algorism to probe the details of the modulated structures, due to the impossibility of choosing a lattice size and boundary condition along the axial direction which do not affect the periodicity of the modulation. For such purpose, therefore, the site dependent molecular field calculation is now in progress.

Acknowledgments

The authors thank the Computer Center, Kyusu University for the use of FACOM M-780/20.

Appendix

By means of the molecular-field approximation the wavevector dependent susceptibility $\chi(\boldsymbol{q})$, is calculated. Letting a lattice constant be unity,

$$\chi(\boldsymbol{q})=\frac{C}{T-T(\boldsymbol{q})} \tag{A1}$$

$$C=Na(g\mu_B)^2 \tag{A2}$$

$$T(\boldsymbol{q})=a[2J_0(\cos q_x+\cos q_y)+2J_1\cos q_z+2J_2\cos 2q_z+2aJ_3\cos 2q_z] \tag{A3}$$

are obtained, where $a=S(S+1)/3=\frac{2}{3}$ for $S=1$, g and μ_B denote the g-factor and the Bohr magneton respectively. By lowering the temperature from the paramagnetic state, the ordered state corresponding to the critical wavevector $\boldsymbol{q}_c$, for which equation (A3) becomes maximum, appears at the beginning. The critical wavevector $\boldsymbol{q}_c=(q_x^c, q_y^c, q_z^c)$ is calculated for $\kappa_0=J_0/J_1>0$ and $\kappa=\kappa_2+a\kappa_3<0$. For $-\frac{1}{4}<\kappa$, $q_x^c=q_y^c=q_z^c=0$ (ferromagnetic phase) and for $\kappa<-\frac{1}{4}$, $q_x^c=q_y^c=0$ and $q_z^c=\cos^{-1}(-1/4\kappa)$ (modulated phase) are obtained (figure 3). Let $T(\boldsymbol{q}_c)$ in each case be T_c and T_m, respectively, then

$$\frac{T_c}{aJ_1}=4\kappa_0+2(1+\kappa) \tag{A4}$$

$$\frac{T_m}{aJ_1}=4\kappa_0-2\left(\kappa+\frac{1}{8\kappa}\right) \tag{A5}$$

and the Lifshitz point is given by

$$\kappa^*=-\tfrac{1}{4} \qquad \frac{T^*}{aJ_1}=4\kappa_0+\tfrac{3}{2}. \tag{A6}$$

The transition temperature T_U defined in section 3 corresponds to T_c for $\kappa>\kappa^*$ and T_m for $\kappa<\kappa^*$, respectively. The cases of the [2-2] and [3-4] model are summarized in table 1.

References

[1] Elliot R J 1961 *Phys. Rev.* **124** 346–53
[2] Bak P and von Boehm J 1980 *Phys. Rev.* B **21** 5297–308
[3] Habenschuss M, Stassis C, Sinha S K, Deckmann H W and Spedding F H 1974 *Phys. Rev.* B **10** 1021–6
[4] Rossat-Mignod J, Burlet P, Bartholin H, Vogt O and Lagnier R 1980 *J. Phys. C: Solid State Phys.* **13** 6381–9
[5] Yokoi C S O, Coutinho-Filho M D and Salinas S R 1981 *Phys. Rev.* B **24** 4047–61
[6] Selke W and Fisher M E 1979 *Phys. Rev.* B **20** 257–65
[7] Render S and Stanley H E 1977 *J. Phys. C: Solid State Phys.* **10** 4765–84
[8] Oitmaa J 1985 *J. Phys. A: Math. Gen.* **18** 365–75
[9] Iwashita T and Uryû N 1979 *J. Phys. Soc. Japan* **47** 786–9. See also other references cited therein
[10] Idogaki T and Uryû N 1985 *Phys. Lett.* **110A** 467–9
[11] Nakanishi K 1989 *J. Phys. Soc. Japan* **58** 1296–306
[12] Thompson C J 1972 *Phase Transitions and Critical Phenomena Vol 1* ed C Domb and M S Green (New York: Academic) pp 177–226
[13] Binder K 1979 *Monte Carlo Method in Statistical Physics* ed K Binder (Berlin: Springer) pp 1–45
[14] Binder K and Heermann D W 1988 *Monte Carlo Method Simulation in Statistical Physics* (Berlin: Springer)
[15] Mo Z and Ferer M 1991 *Phys. Rev.* B **43** 10890–905